Heliyon 11 (2025) e41857

Contents lists available at ScienceDirect

Heliyon

journal homepage: www.cell.com/heliyon

Research article

Highly sensitive non-enzymatic glucose sensing using Ni nanowires and graphene thin film on the gate area of extended gate electric double-layer field-effect transistor

Sheng-Chun Hung

Department of Electrical Engineering, Feng Chia University, Taichung, 407802, Taiwan

ARTICLE INFO

Keywords:
Glucose sensors
Ni nanowires
Graphene
Electric double layer (EDL)
Field-effect transistors (FETs)

ABSTRACT

This study presents an innovative glucose detection platform, featuring a highly sensitive, non-enzymatic glucose sensor. The sensor integrates nickel nanowires and a graphene thin film deposited on the gate region of an extended-gate electric double-layer field-effect transistor (EGEDL-FET). This unique combination of materials and device structure enables superior glucose sensing performance. Ni nanowires were deposited on the surface of the extended gate region of the EGEDL-FET, where high quality monolayer graphene grown by chemical vapor deposition (CVD) had been previously transferred. The Ni nanowires provide a high surface area and excellent catalytic activity for non-enzymatic glucose oxidation. Meanwhile, the graphene thin film enhances the conductivity of the sensing interface due to the matching of work functions between the Ni nanowires and the graphene. The bimetal gate-electrolyte interface with a spacing of 65 μm forms an electric double layer that effectively avoids ion shielding due to its dimension being smaller than the Debye length. This configuration significantly amplifies the electrical signal, thereby enhancing the sensor's sensitivity. The fabricated EGEDL-FET glucose sensor demonstrates a wide linear range from 0.05 mM to 5 mM, high sensitivity of 1043 mA μM^{-1} cm^{-2}, and a low detection limit of 51 nM. The synergistic effect of the Ni nanowires, graphene film, and EGEDL-FET configuration results in a highly sensitive non-enzymatic glucose sensor with excellent selectivity in glucose alkaline solutions containing both chloride ions and potassium ions. These experimental results represent a promising advancement for glucose monitoring systems, offering improved performance and reliability.

1. Introduction

Diabetes has emerged as one of the fastest-growing chronic diseases in the 21st century, with a significant increase in prevalence worldwide [1]. This metabolic disorder occurs when the pancreas fails to produce sufficient insulin or the body cannot effectively utilize the insulin it generates. Over time, the persistent hyperglycemia associated with diabetes can severely damage various bodily systems, particularly the nerves and blood vessels.

Recent estimates suggest that the global burden of diabetes is staggering and continues to rise at an alarming rate. In 2014, 8.5 % of adults aged 18 years and older were affected by diabetes. By 2019, the International Diabetes Federation (IDF) reported that 463 million adults were living with diabetes globally, a figure that has increased by 38 million since 2017. Projections indicate that the

---

E-mail address: schunhung@o365.fcu.edu.tw.

https://doi.org/10.1016/j.heliyon.2025.e41857
Received 16 September 2024; Received in revised form 8 January 2025; Accepted 8 January 2025

number of people with diabetes will further escalate to 578 million by 2030 and 700 million by 2045.

Type 2 diabetes, which accounts for 90 % of all diabetes cases, is largely preventable and potentially reversible if identified and managed early in the disease course. However, the increasing prevalence of obesity, driven by multiple factors, has contributed to the rise in type 2 diabetes worldwide [2]. Preventing and controlling this disease remains an ongoing challenge, as it requires a better understanding of disparities in risk factor profiles and diabetes burden across populations to inform effective strategies.

The global burden of diabetes extends beyond its high prevalence, as it is a major cause of mortality, morbidity, and significant health care expenditures. Uncontrolled diabetes can lead to various complications, including microvascular disease, retinopathy, nephropathy, neuropathy, and macrovascular disease (atherosclerosis), which increase the risk of heart disease, stroke, blindness, kidney failure, and limb amputation.

Ultimately, Diabetes has emerged as a defining disease of the 21st century, with its prevalence and associated complications presenting a significant global health challenge. Addressing this epidemic necessitates a multifaceted approach, including population-based prevention strategies, early identification, and effective management. Prioritizing research and implementing evidence-based interventions are crucial steps to mitigate the impact of diabetes and enhance health outcomes for affected individuals.

Glucose detection can be achieved through various mechanisms, including thermal [3], optical [4], electrochemical [5], acoustic [6], and magnetic methods [7]. Among these, electrochemical methods are the most widely researched, involving the enzymatic oxidation of glucose, which leads to the measurement of electron flow to quantify glucose concentration.

The development of glucose sensors can be broadly divided into three generations. First-generation enzyme-based glucose sensors, developed by Clark and Lyons, monitor the hydrogen peroxide produced during the glucose oxidase (GOx) catalyzed oxidation process. Despite poor accuracy due to oxygen consumption, improvements like dual cathodes have been made [8–13]. Second-generation sensors use artificial electron transfer mediators instead of oxygen, but face issues like poor reproducibility and mediator toxicity [14]. Third-generation sensors promote direct electron transfer using nanostructures to connect the FAD active center of GOx to the electrode, reducing interference and enhancing biocompatibility [15–19]. Non-enzymatic glucose sensors employ electrocatalysts instead of enzymes, addressing limitations of enzymatic sensors like pH range and temperature sensitivity [20]. Current blood glucose measurement methods involve finger pricks, causing discomfort and failing to provide real-time monitoring. To address these limitations, minimally invasive and non-invasive continuous glucose monitoring (CGM) technologies are being developed, offering real-time glucose data without repeated finger pricks. These advancements in glucose monitoring aim to improve diabetes management and patient quality of life.

In this study, we present the use of high-quality graphene, grown through chemical vapor deposition (CVD), in combination with nickel nanowires as gate electrode materials for the development of field-effect transistor (FET) sensors with electrical double-layer gates. The CVD-grown graphene serves a dual function: it acts as a supporting substrate for the nickel nanowires and provides a conductive pathway that mitigates electron neutralization caused by material defects. Furthermore, in the DMOS FET configuration, the contact between the N-type channel and the P-type substrate induces spontaneous polarization within the P-type substrate, thus creating an electric field directed toward the N-type channel. This electric field enhances the attraction of electrons from the N-type region to the interface, resulting in a substantial accumulation of electrons at this interface, which forms a two-dimensional electron gas (2DEG) [21,22]. The FET architecture promotes strong spontaneous polarization, leading to the establishment of a two-dimensional electron density. Additionally, when an external electric field is applied by introducing a positive gate voltage ($V_{GS} > 0$), this external influence interacts with the internal electric field generated by spontaneous polarization. This interplay further increases the electron density within the N-type channel as more electrons are drawn into this region. Such interaction not only enhances carrier mobility but also improves the overall performance of the sensor. Consequently, minor changes in surface potential have a direct impact on this electron density, which is further amplified by variations in the device current. To effectively convert and amplify the glucose concentration in the solution into an electrical signal, this study employs an electrical double-layer field-effect transistor (EDL FET) design. The adjustable electrical double-layer spacing allows precise control of the ion capacitance spacing in the solution, which can be modulated by the external gate voltage. This approach surpasses the theoretical Debye length limit and lowers the detection limit [23–26]. The configuration, which utilizes a graphene-nickel nanowire composite material as the gate electrode of the EDL FET sensor, offers significant advantages for low-concentration glucose detection, achieving both a low detection limit and high selectivity. This study successfully demonstrates a glucose detection limit as low as 51 nM, along with excellent interference immunity in environments containing potassium and sodium ions.

2. Material and methods

2.1. Fabrication and characterization of Ni nanowire

The chemicals necessary for the synthesis of nickel nanowires included nickel (II) chloride hexahydrate (NiCl2·6H2O; 99.9 %), ethylene glycol (EG; 99.8 %), hydrazine monohydrate (N2H4·H2O; 98 %), and poly(vinylpyrrolidone) (PVP; Mw 40,000). These were sourced from Sigma-Aldrich (St. Louis, MO, USA). Ultrapure deionized water (DI; Millipore water systems) with a resistivity of 18.2 MΩ cm^{-1} was utilized throughout the experiments. All chemicals were employed as received, without any further purification.

To synthesize nickel nanowires, we combined 75 μL of a 1 M $NiCl_2$ aqueous solution with 15 mL of ethylene glycol (EG) and heated the mixture to 100 °C. Following this, we carefully added 0.5 mL of hydrazine monohydrate ($N_2H_4 \cdot H_2O$) dropwise into the heated solution. The reaction was allowed to proceed at this temperature for approximately 30 min, during which a dark gray product formed and floated on the surface.

The resulting product was washed several times with deionized water and absolute ethanol using magnetic decantation. It was then

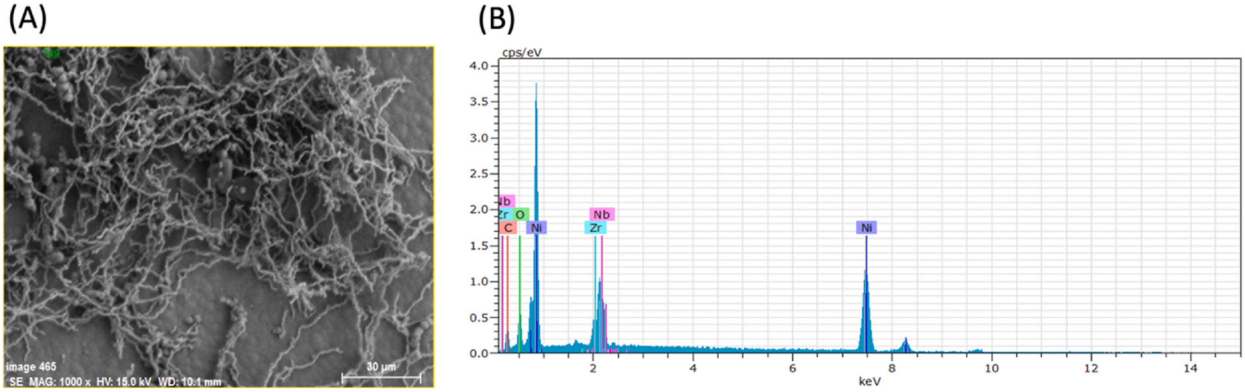

Fig. 1. (A) Scanning Electron Microscopy (SEM) image illustrating the deposition of nickel (Ni) nanowires on a metal pad. (B) Energy Dispersive Spectroscopy (EDS) results pertaining to the Ni nanowires positioned on the metal pad.

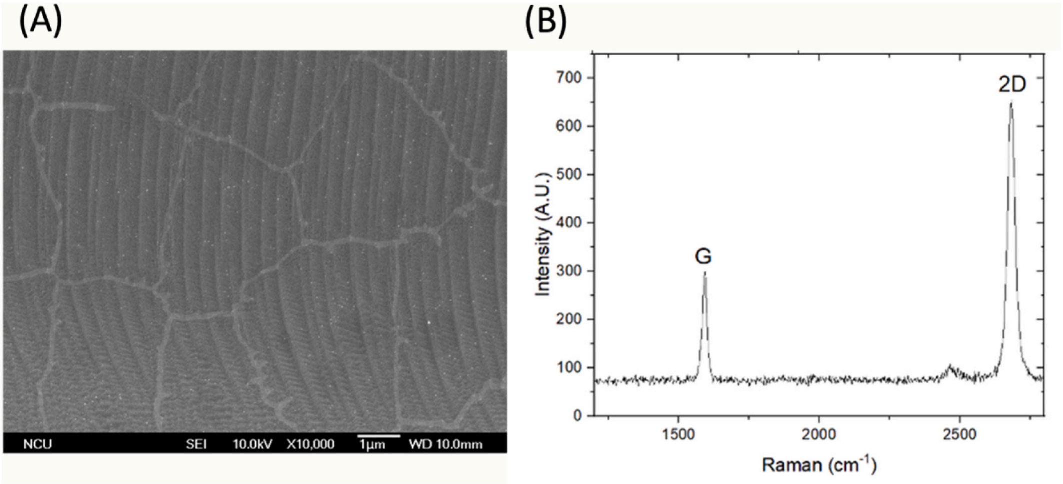

Fig. 2. (A) Scanning Electron Microscopy (SEM) image of a graphene thin film deposited on copper foil. (B) Raman spectroscopy analysis of the graphene thin film situated on a metal pad.

dispersed in ethanol for subsequent characterization. The synthesized nickel nanowires suspended in ethanol were applied to the double-electrode metal pad of the extended gate using a micropipette.

For characterization purposes, scanning electron microscopy (SEM) and energy dispersive X-ray spectroscopy (EDS) were employed. The SEM images, shown in Fig. 1(A), were obtained with a JEOL JEM6390 SEM (Tokyo, Japan), while the EDS patterns in Fig. 1(B) were acquired using a Bruker XFlash Detector 4010 (Billerica, MA, USA) integrated into the SEM.

2.2. *Fabrication and characterization of graphene thin film*

The single-layer graphene employed in the glucose sensor was synthesized on 25 μm thick copper foil using chemical vapor deposition (CVD). The growth process was conducted within a quartz tube furnace, utilizing methane and hydrogen as precursor gases. The furnace was heated with a hydrogen flow of 2 sccm under a vacuum of 10 mTorr, maintaining a growth temperature of 1000 °C. After annealing the copper foil for 40 min to facilitate recrystallization, a methane flow of 35 sccm was introduced, with growth durations ranging from 30 s to 15 min. Following this, a rapid cooling method (300 °C/min) was applied, with the continuous flow of methane and hydrogen sustained throughout the cooling process.

To characterize the graphene films on the copper foil, scanning electron microscopy (SEM) was employed. The graphene film was subsequently transferred to the metal surface of the extended gate using a polymethylmethacrylate (PMMA) coating along with iron (III) nitrate etching. The transferred graphene film was then further analyzed using Raman spectroscopy.

Fig. 2 (A) presents an SEM image of the graphene grown on copper foil, illustrating visible copper grains, continuous graphene films, copper surface steps, and graphene wrinkles. Raman spectroscopy was utilized to evaluate the quality and uniformity of the graphene on the extended gate metal substrates. The Raman spectra shown in Fig. 2 (B), especially the D and 2D bands, provide detailed insights into defect density and film thickness. The Raman spectrum depicted in Fig. 2 (B) exhibits characteristic features of

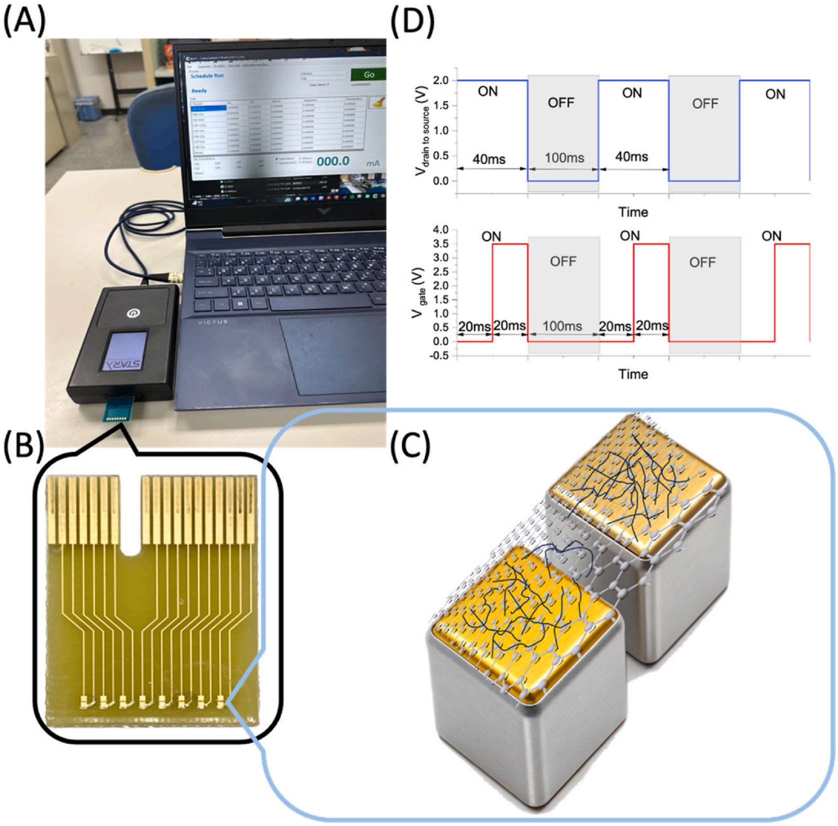

Fig. 3. (A) The entire system comprises a sensor chip, a reader, and a user interface presented on a laptop computer. (B) The sensor chip features eight individual sensors organized in a 1x8 array. (C) This illustrates a schematic diagram of the Ni nanowires/graphene within the sensing area. (D) A square wave of gate and drain voltage (20 ms on/20 ms off) is applied to the sensor electrode, with a 100 ms off-state interval.

single-layer graphene: (1) a G-2D intensity ratio of 0.5 and (2) a symmetric 2D band centered at 2680 cm^{-1} with a full width at half maximum of 26 cm^{-1}. The randomly collected Raman spectra from this area indicate that high-quality single-layer graphene has been uniformly transferred to the extended gate metal substrate.

2.3. Manufacturing process steps of extended gate chip

The innovative glucose detection platform features a sophisticated sensor chip with gold electrodes, manufactured by STARX Co. in Taiwan on a printed circuit board (PCB). This sensor chip consists of an array of eight individually addressable sensors arranged in a 1 × 8 configuration. To delineate the sensing area for metal deposition, UV photolithography was employed. The metal layers were applied using electron beam evaporation, following a sequential structure of 200 Å of titanium (Ti), 500 Å of gold (Au), 500 Å of platinum (Pt), and 2000 Å of gold (Au). Following the metal deposition, the device was passivated with a photoresist layer, and additional photolithography was utilized to create two open regions on the gold electrodes. One sensing electrode was connected to the gate terminal of the MOSFET, while the other was linked to the reference electrode, where the gate bias was applied. In this study, we employed an adjustable-spacing planar electric double-layer structure to enhance the sensitivity of glucose detection. We drew upon the research conducted by Yi-Ting et al., published in Scientific Reports in 2018 [26], which demonstrated that, at a fixed voltage, the current gain declines as the distance between the gate electrode and the FET channel increases, until a saturation region is reached. Within this region, the characteristics of the electric double layer are determined solely by the gate voltage and remain unaffected by changes in spacing. This behavior is consistent with traditional potentiometric theory, where the sensitivity in this region corresponds to the theoretical values outlined in the Nernst equation (RT/nF). Furthermore, operating in the linear region, where the current gain increases as the spacing decreases, allows for sensitivity levels that exceed those predicted by the Nernst equation. With this in mind, we designed the sensing electrode area to measure 600 μm × 600 μm, with a gap of 65 μm between the two open areas, thereby establishing the planar electric double-layer spacing at 65 μm. Fig. 3 presents a photograph of the extended gate wafer alongside a schematic diagram of the measurement device. It features a total of eight channels, enabling simultaneous experimentation to minimize errors.

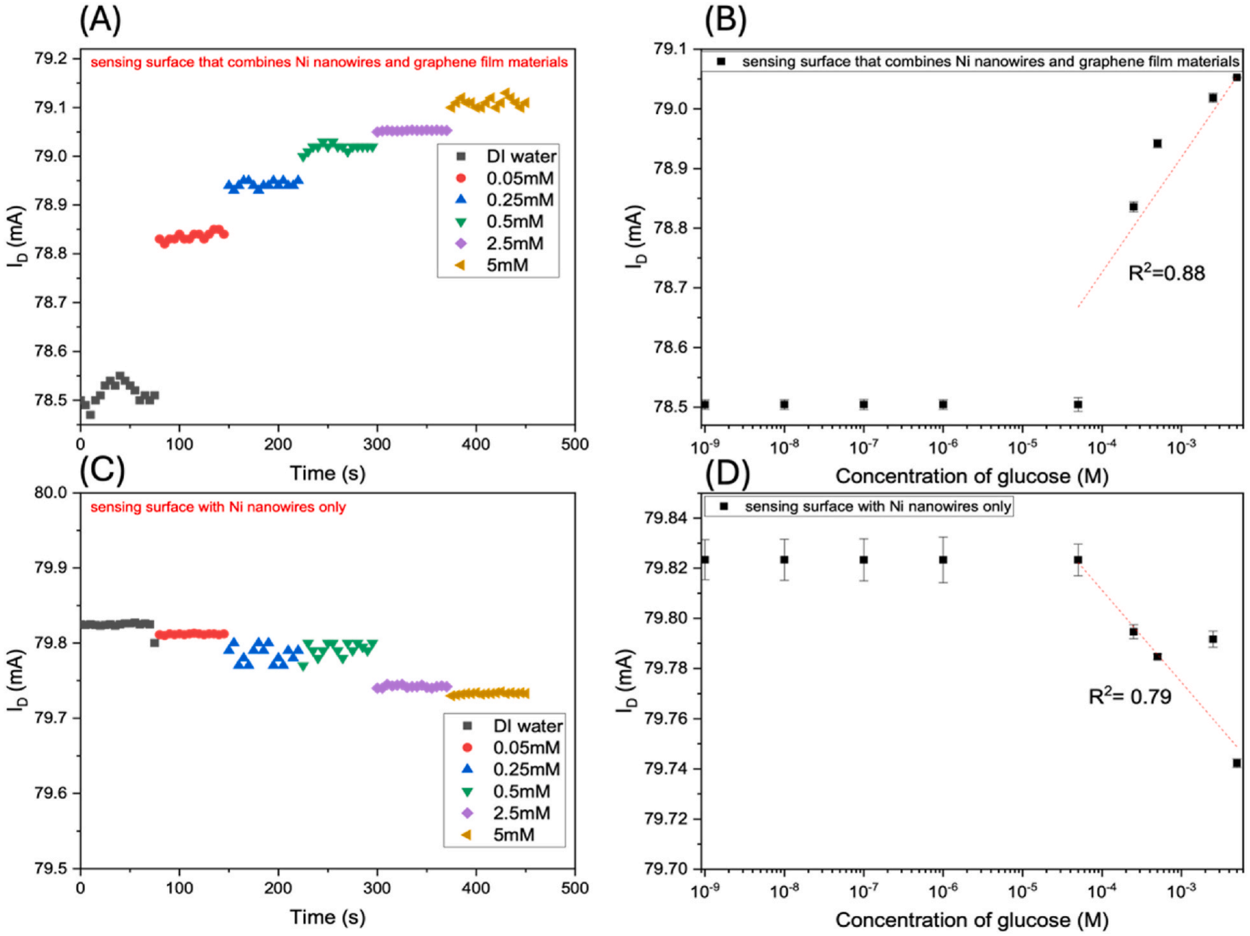

Fig. 4. (A) Variation in drain current of a Ni nanowire-decorated graphene-gated glucose sensor as a function of glucose concentration. (B) Change in drain current for a Ni nanowire-decorated graphene-gated glucose sensor in response to glucose concentration. (C) Variation in drain current of a Ni nanowire-decorated gated glucose sensor as a function of glucose concentration. (D) Change in drain current of a Ni nanowire-decorated gated glucose sensor as influenced by glucose concentration.

2.4. Fabrication of nickel nanowire-graphene composite on extended gate sensor chip

The preparation of nickel nanowire-graphene composite materials on extended gate sensor wafers involves a series of steps. Initially, a graphene film, grown through chemical vapor deposition (CVD), is transferred onto the substrate. A layer of polymethylmethacrylate (PMMA) is then applied to the graphene surface, and the underlying copper film is oxidized to form cuprous oxide. This oxidation is essential as it minimizes the coupling between the copper and the graphene. Electrolysis in a sodium hydroxide (NaOH) solution is subsequently conducted to generate hydrogen gas, which facilitates the separation of the graphene from the copper. Following this, the PMMA/graphene layer is transferred onto the extended gate sensor wafer, and acetone is used to dissolve and remove the PMMA. To deposit nickel nanowires onto the graphene films, a solution containing nickel nanowires uniformly dispersed in acetone is applied to the graphene film in the gate area using a micropipette. The samples are then baked in an oven at 150 °C for 40 min, a process that helps remove any excess moisture and promotes van der Waals adhesion of the nickel nanowires to the graphene film.

3. Results and discussion

3.1. Measurement

In this study, N-channel depletion mode DMOS FETs and extended gate dies were employed as measurement elements. Glucose solutions of varying concentrations were applied to the sensing electrode area using a micropipette. During the test, a pulse bias voltage was applied to the reference electrode, and the sensing electrode was connected to the gate of the transistor via the extended gate. For voltage settings, a drain-to-source voltage of 2V was used, with gate pulse voltages of 0V and 3.5V applied for a pulse duration

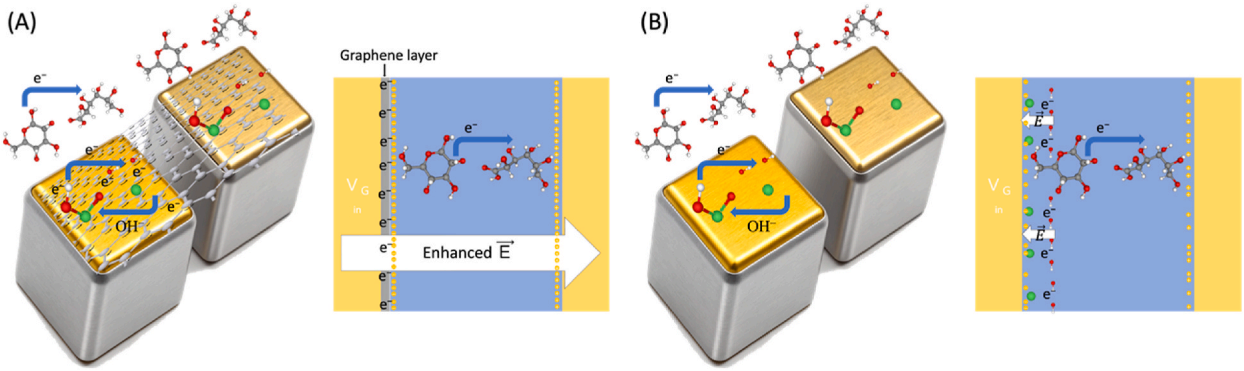

Fig. 5. (A) depicts a schematic representation of a metal electrode integrated with graphene and nickel nanowires. The diagram on the right illustrates the role of the graphene layer in enhancing charge accumulation and facilitating the transmission of the electric field. (B) presents a schematic of a metal electrode composed solely of nickel nanowires. The corresponding illustration on the right indicates that, although electrons are released during the redox reaction, they become trapped in defects within the nanowire structure. This results in the formation of a partial reverse electric field, hindering efficient charge distribution.

of 20 ms, and the drain current was measured.

The measurement results are illustrated in Fig. 4. Fig. 4 (A) presents the variations in current over time for glucose solutions of different concentrations. After allowing the chip to stabilize in a deionized water environment, a solution with a glucose concentration of 0.05 mM was introduced at the 75-s mark, leading to a rapid increase in current. Subsequently, glucose solutions with concentrations of 0.25, 0.5, 2.5, and 5 mM were added sequentially, each causing a proportional rise in sensor current.

Fig. 4 (B) demonstrates the measured drain current as a function of glucose concentration, revealing a linear relationship. This linear behavior can be attributed to the electrochemical transformation of nickel (Ni) nanowires during the redox reaction with glucose molecules in an alkaline solution, resulting in the formation of a $Ni(OH)_2$/NiOOH redox couple. This reaction generates a substantial number of electrons, which, when a gate voltage is applied, polarize the molecules in the solution. This polarization establishes an electric double layer in the dual-electrode sensing area. The generated charges are rapidly and uniformly transferred through the underlying graphene to the extended gate metal surface, enhancing the negative charge in the electric double layer (EDL) and thereby increasing the positive potential (ΔVg) at the opposite end.

According to the parallel plate capacitor model, the change in gate voltage can be expressed by the equation

$$\Delta Vg = (\Delta\sigma)d/\epsilon$$

The Gouy-Chapman theory indicates that the increase in surface charge density is directly proportional to the glucose concentration in the solution. Consequently, changes in the gate bias lead to a linear relationship between the drain-source current and the glucose concentration.

Based on the results presented in Fig. 4(B), the sensor demonstrates a sensitivity of 3102.7 μA mM^{-1} cm^{-2} and achieves a detection limit (LOD) of 51 nM. The LOD was calculated using the formula:

$$LOD = \frac{3.3\sigma}{S}$$

where S represents the sensitivity and $\sigma\sigma$ denotes the standard deviation of the lowest measured concentration. The calculated LOD of 51 nM corresponds to approximately 3.07×10^{17} $ions/m^3$.

Additionally, using the Debye length calculation formula:

$$\lambda_D = \sqrt{\frac{\varepsilon k_B T}{nq^2}}$$

where ε_r (relative permittivity) of deionized water is 81, we calculated the Debye length to be approximately 194 μm. In contrast, the metal spacing designed in our experiment is only 65 μm. This result indicates that the proposed planar electric double-layer structure is capable of effectively transmitting the influence of the applied electric field within this range, thereby mitigating the limitations caused by charge screening effects on the detection limit.

In a control experiment, nickel nanowires were directly deposited onto the gold surface of the extended gate, without transferring graphene onto the gate metal. The glucose detection experiment was subsequently repeated. As illustrated in Fig. 4(C) and (D), when the nickel nanowires come into direct contact with the alkaline solution on the gold surface, the $Ni(OH)_2$/NiOOH redox pair forms on the surface of the nanowires. However, when this redox pair interacts with glucose molecules in the solution, the released electrons result in a decrease in the gate potential. Furthermore, the significant difference in work function between the nickel nanowires and the gold surface inhibits the effective distribution of electrons across the surface. Consequently, while electrons are generated, they are

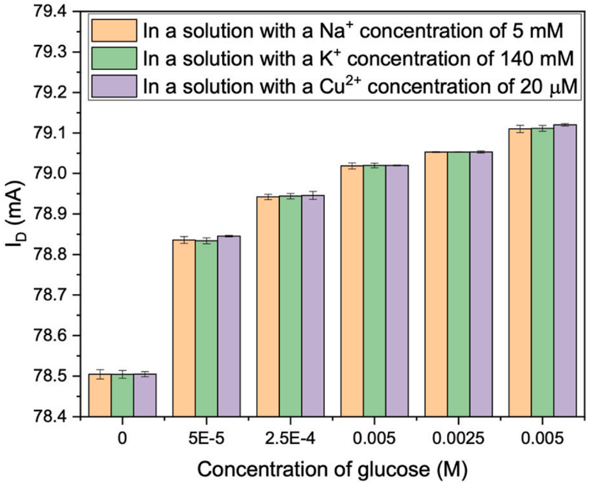

Fig. 6. The evaluation of interference resistance for a glucose sensor utilizing nickel nanowire and graphene hybrid electrodes was conducted in the presence of sodium, potassium, and copper ions.

captured by defects within the polycrystalline structure of $Ni(OH)_2$, preventing them from exerting a significant influence on the gate surface potential. This leads to the formation of a partial back electric field internally, which diminishes the overall potential of the gate. Therefore, although minor changes in potential can be observed, their magnitude is considerably less than the effects produced by the nickel nanowires on the graphene film. As illustrated in Fig. 5, when glucose molecules interact with the $Ni(OH)_2$/NiOOH redox pair, the resulting electrons are rapidly distributed across the graphene film. This efficient distribution enhances the original electric field, effectively improving the overall sensing performance. This comparative evidence verifies that the graphene and nickel nanowire composite materials used in this experiment have closely matched work functions and that graphene's excellent electrical properties effectively facilitate the charge transfer of electrons generated by the redox reactions of glucose and nickel nanowires. This enhances the signal amplification, confirming the superior performance of the composite materials in glucose detection.

3.2. Glucose detection mechanism of Ni nanowires and graphene thin film on the extended gate of an electric double-layer field-effect transistor

The reaction mechanism utilized in this study is outlined as follows:

When Ni nanowires are immersed in an alkaline solution, the hydroxide ions (OH^-) induce electrochemical transformation, forming an active $Ni(OH)_2$/NiOOH redox pair on the nanowire surface. This reaction is represented by the equation:

$$NiO(OH) + H_2O + e^- \leftrightarrow Ni(OH)_2 + OH^-$$

Simultaneously, glucose molecules are oxidized to gluconic acid by $Ni(OH)_2$, as described by the following reaction:

$$Ni(OH)_2 + \text{glucose} \leftrightarrow NiO(OH) + \text{gluconic acid} + H^+ + e^-$$

The amorphous nature of the $Ni(OH)_2$ layer introduces a high degree of structural disorder and incompleteness, significantly enhancing the electrochemical efficiency compared to Ni single crystal. However, this amorphous structure also creates numerous defect centers that easily capture electrons. Due to the small work function of amorphous $Ni(OH)_2$, approximately 4.42 eV, a graphene film with a similar work function (also about 4.42 eV) was utilized in this experiment. This small work function is beneficial for efficient electron transfer during glucose oxidation. The high conductivity of graphene allows for the rapid dispersion of electrons generated by glucose oxidation, forming an electron-rich layer on the surface of the extended gate wafer. This affects the original gate bias voltage and alters the electron channel width in the transistor. The combination of the small work function of amorphous $Ni(OH)_2$ and the high conductivity of the graphene film synergistically enhances glucose detection performance. The $Ni(OH)_2$ layer provides active sites for glucose oxidation, while the graphene film effectively conducts the electrical signals generated by the redox reaction. This synergy is critical for the glucose detection mechanism.

This study further investigated the specificity and anti-interference capabilities of glucose detection by selecting sodium ions (Na^+), potassium ions (K^+), and copper ions (Cu^{2+}) as the primary interference parameters for analysis. Sodium, the predominant cation in extracellular fluid, plays a vital role in regulating osmotic pressure, fluid balance, and blood pressure. Variations in sodium concentration can significantly affect plasma osmotic pressure and intracellular water movement, particularly under pathological conditions such as hyperglycemia or dehydration. Conversely, potassium, the primary cation in intracellular fluid, is essential for maintaining membrane potential and modulating the excitability of nerves and muscles. Abnormal fluctuations in potassium levels can deeply impact cardiac function and other critical physiological processes, underscoring its clinical importance for monitoring. Copper ions (Cu^{2+}) are vital trace elements necessary for the proper functioning of numerous enzymes. An adult body typically contains

Table 1
Summary of various techniques used by different research teams for accurately detecting glucose levels.

Detection Method	Detection Limit	Materials	Reference
Lead ion selective membrane (Pb-ISM) coated AlGaN/GaN HEMT	2 mM	AlGaN/GaN high electron mobility transistors (HEMT)	[26]
Nanocomposite of reduced graphene oxide and gold nanoparticles	0.5 mM	Reduced graphene oxide, gold nanoparticles	[32]
Electrochemical sensor based on hierarchical porous carbon	1 μM	Hierarchical porous carbon	[33]
Flexible and stretchable electrochemical sensors	10 μM	Various flexible materials (review)	[34]
Electrochemical sensor based on metal-organic framework composite	5 μM	Metal-organic frameworks	[35]
Review of microfluidic devices for point-of-care testing	50 nM	Various microfluidic materials (review)	[36]
Electrochemical sensor based on graphene oxide-modified electrode	100 μM	Graphene oxide	[37]
Review of advances in electrochemical sensors for glucose detection	1 μM	Various electrochemical materials (review)	[38]
Review of wearable biosensors for glucose monitoring	20 nM	Various wearable biosensor technologies (review)	[39]
Review of advances in electrochemical sensors for glucose detection	5 μM	Various electrochemical materials (review)	[40]
Electrochemical biosensor based on enzyme immobilization on graphene oxide-modified electrode	50 μM	Graphene oxide, enzymes	[41]
Review of recent advances in electrochemical sensors for glucose detection	1 μM	Various electrochemical materials (review)	[42]
Review of nanomaterials for drug delivery	15 nM	Various nanomaterials (review)	[43]
Review of advancements in electroanalysis of glucose using nanomaterials	0.1 mM	Various nanomaterials (review)	[44]
nickel nanowire and graphene hybrid electrodes on EDL-FET	51 nM	nickel nanowire and graphene hybrid electrodes	This study

approximately 100–200 mg of copper, most of which is bound to ceruloplasmin in the plasma, which carries around 95 % of plasma copper. Copper plays a significant role in various key biochemical processes, including redox reactions, iron metabolism, and antioxidant defense systems; thus, its stability is crucial for maintaining normal physiological functions. Under normal circumstances, even during physiological challenges such as dehydration or hyperglycemia, the concentrations of sodium, potassium, and copper in the body remain stable within predictable ranges. Moreover, compared to glucose, the levels of these electrolytes in sweat and other bodily fluids are less susceptible to external environmental factors, such as temperature variations or physical activity [27–31]. This consistency in measurement further emphasizes the reliability of sodium, potassium, and copper ions as physiological indicators, even following exercise or periods of significant sweating.

In this study, we utilized typical concentrations of sodium ions (Na^+), potassium ions (K^+), and copper ions (Cu^{2+}) found in healthy human blood—5 mM, 140 mM, and 20 μM, respectively—as interference parameters to assess glucose solutions with varying concentrations. The findings, depicted in Fig. 6, demonstrate that the glucose sensor, which employs nickel nanowires in conjunction with graphene as the gate material, exhibits remarkable anti-interference performance.

Table 1 demonstrates that numerous research teams have effectively employed a range of methods to detect glucose concentrations. These methods encompass non-enzymatic electrochemical techniques, wearable sensor technology, enzyme immobilization electrochemical methods, microfluidic technology, and near-infrared spectroscopy, among others. Each of these approaches has yielded commendable results. In this study, we present an innovative method that integrates nickel (Ni) nanowires and graphene within an electric double layer and field-effect transistor (FET) structure. This novel approach allows for the development of a glucose sensor that features rapid response times and a low detection limit.

4. Conclusion

The experimental data from this study reveal that we successfully employed an extended gate wafer featuring a planar dual-electrode spacing to control the thickness of the electric double layer (EDL). With a spacing of 65 μm, we achieved a detection limit of 51 nM, corresponding to a Debye length of 194 μm for glucose at this concentration in deionized water. These results confirm that our proposed structural design enables the glucose sensing element to surpass the theoretical limits established by the Nernst equation.

In addition, the hybrid electrode structure, composed of nickel nanowires and graphene—both of which possess similar work functions—significantly enhanced the number of electrons generated from the electrochemical redox reactions of the nickel nanowires in a weakly alkaline glucose solution. These electrons were effectively distributed across the extended gate metal pad. Driven by the electric double-layer capacitance effect, the gate surface potential modulated the electron channel width of the field-effect transistor, ultimately producing an amplified current readout through the transistor.

This innovative sensor design demonstrates high sensitivity, a low detection limit, and excellent linearity across a glucose concentration range of 0.05 mM–5 mM. Moreover, the nickel nanowire-graphene hybrid structure showcases remarkable reproducibility and resistance to interference. By integrating the EGEDL-FET wafer with the nickel nanowire-graphene hybrid electrode, this research has developed a high-performance glucose sensing platform that effectively overcomes the limitations of the Nernst equation by utilizing the small electrode spacing of the electric double layer. This advancement significantly contributes to the development of minimally invasive, non-enzymatic blood glucose monitoring devices.

Data availability statement

Data will be available on the request from the corresponding author.

Funding statement

This research was funded by Taiwan's MOST grant 110-2222-E−035-010-MY2 and Feng Chia University's 112 Academic Year Research Leap Project 23H00809.

Declaration of competing interest

The author declare that there are no competing financial interests or personal relationships that could have influenced the work reported in this paper.

Acknowledgments

The measuring instruments used in this study were partially provided by Taiwan's STARX.

References

[1] E. Standl, K. Khunti, T.B. Hansen, O. Schnell, The global epidemics of diabetes in the 21st century: current situation and perspectives, European Journal of Preventive Cardiology 26 (2_suppl) (2019) 7–14, https://doi.org/10.1177/2047487319881021.
[2] M.D. Butt, S.C. Ong, A. Rafiq, T. Malik, A. Sajjad, N. Batool, A.U.H. Chughtai, M.U. Wahab, M. Abdullah, Z.-U.-D. Babar, An observational multi-center study on type 2 diabetes treatment prescribing pattern and patient adherence to treatment, Sci. Rep. 13 (1) (2023) 1, https://doi.org/10.1038/s41598-023-45767-6.
[3] M. Caldara, J.W. Lowdon, R. Rogosic, R. Arreguin-Campos, K.L. Jimenez-Monroy, B. Heidt, K. Tschulik, T.J. Cleij, H. Diliën, K. Eersels, B. van Grinsven, Thermal detection of glucose in urine using a molecularly imprinted polymer as a recognition element, ACS Sens. 6 (12) (2021) 4515–4525, https://doi.org/10.1021/acssensors.1c02223.
[4] E.Y. Park, J. Baik, H. Kim, others, Ultrasound-modulated optical glucose sensing using a 1645 nm laser, Sci. Rep. 10 (2020) 13361, https://doi.org/10.1038/s41598-020-70305-6.
[5] A. Heller, B. Feldman, Electrochemical glucose sensors and their applications in diabetes management, Chem. Rev. 108 (7) (2008) 2482–2505, https://doi.org/10.1021/cr068123g.
[6] A. Aloraynan, S. Rassel, C. Xu, D. Ban, A single wavelength mid-infrared photoacoustic spectroscopy for noninvasive glucose detection using machine learning, Biosensors 12 (3) (2022) 166, https://doi.org/10.3390/bios12030166.
[7] J. Hanna, Y. Tawk, S. Azar, others, Wearable flexible body matched electromagnetic sensors for personalized non-invasive glucose monitoring, Sci. Rep. 12 (2022) 14885, https://doi.org/10.1038/s41598-022-19251-z.
[8] L.C. Clark Jr., C. Lyons, Electrode systems for continuous monitoring in cardiovascular surgery, Ann. N. Y. Acad. Sci. 102 (1962) 29–45, https://doi.org/10.1111/j.1749-6632.1962.tb13623.x.
[9] H.J. Lee, H. Choi, Y.-I. Jin, K.-Y. Hwang, D.-C. Park, S. Min, Effect of nozzle inlet geometry in high temperature hydrocarbon liquid jets, Int. J. Heat Fluid Flow 74 (2018) 1–14, https://doi.org/10.1016/j.ijheatfluidflow.2018.09.004.
[10] B. Noor Aini, S.S. Siddiquee, K. Ampon, K.F. Rodrigues, S. Suryani, others, Development of glucose biosensor based on ZnO nanoparticles film and glucose oxidase-immobilized eggshell membrane, Sensing and Bio-Sensing Research 4 (2015) 46–56, https://doi.org/10.1016/j.sbsr.2015.03.004.
[11] S.J. Updike, G.P. Hicks, The enzyme electrode, Nature 214 (5092) (1967) 986–988, https://doi.org/10.1038/214986a0.
[12] C. Chen, Q. Xie, D. Yang, H. Xiao, Y. Fu, Y. Tan, S. Yao, A review of the electrochemical glucose sensor based on nanomaterials, RSC Adv. 3 (2013) 4473–4491, https://doi.org/10.1039/C3RA22775A.
[13] H. Lee, Y.J. Hong, S. Baik, T. Hyeon, D.H. Kim, Advanced healthcare materials for glucose monitoring: a review, Adv. Healthcare Mater. 7 (1) (2018) 1–14, https://doi.org/10.1002/adhm.201700579.
[14] K. Tian, M. Prestgard, A. Tiwari, Recent advances in materials for glucose biosensors: a review, Mater. Sci. Eng. C 41 (2014) 100–118, https://doi.org/10.1016/j.msec.2014.04.003.
[15] A. Vaze, N. Hussain, C. Tang, D. Leech, J.F. Rusling, Biocatalytic anode for glucose oxidation utilizing carbon nanotubes for direct electron transfer with glucose oxidase, Electrochem. Commun. 11 (10) (2009) 2004–2007, https://doi.org/10.1016/j.elecom.2009.08.039.
[16] J. Wang, Review on glucose sensors, Chem. Rev. 108 (2) (2008) 814–825, https://doi.org/10.1021/cr068123g.
[17] S. Pakapongpan, R.P. Poo-arporn, Self-assembly of glucose oxidase on reduced graphene oxide-magnetic nanoparticles nanocomposite-based direct electrochemistry for reagentless glucose biosensor, Mater. Sci. Eng. C 76 (2017) 398–405, https://doi.org/10.1016/j.msec.2017.03.031.
[18] L. Fang, B. Liu, L. Liu, Y. Li, K. Huang, Electrochemical sensors for glucose detection: a review, Sensor. Actuator. B Chem. 222 (2016) 1098–1104, https://doi.org/10.1016/j.snb.2015.08.032.
[19] K. Hyun, S.W. Han, W.-G. Koh, Y. Kwon, Direct electrochemistry of glucose oxidase immobilized on carbon nanotube for improving glucose sensing, Int. J. Hydrogen Energy 40 (5) (2015) 2199–2206, https://doi.org/10.1016/j.ijhydene.2014.12.019.
[20] D. Bruen, C. Delaney, L. Florea, D. Diamond, Glucose sensing for diabetes monitoring: recent developments, Sensors 17 (8) (2017) 1866, https://doi.org/10.3390/s17081866.
[21] D. Rhee, Reconfigurable SWCNT ferroelectric field-effect transistor arrays, arXiv (2024), https://doi.org/10.48550/arXiv.2411.03198.
[22] D.-G. Jin, S.-G. Kim, H. Jeon, E.-J. Park, S.-H. Kim, J.-Y. Kim, H.-Y. Yu, Improvement of polarization switching in ferroelectric transistor by interface trap reduction for brain-inspired artificial synapses, Mater. Chem. Phys. 258 (2023) 123456, https://doi.org/10.1016/j.matchemphys.2023.123456.
[23] Y. Zhang, J. Wang, L. Chen, Highly sensitive glucose sensors based on enzyme-modified whole-graphene solution-gated transistors, Sci. Rep. 5 (2015) 8311, https://doi.org/10.1038/srep08311.
[24] H. Kim, S. Lee, Electrical double-layer field-effect transistors for biosensing applications: a review, Sensors 19 (19) (2023) 4214, https://doi.org/10.3390/s19194214.
[25] J. Choi, S. Park, Nanomaterial-based biosensors using field-effect transistors: principles and applications, J. Mater. Sci. 57 (4) (2022) 1–20, https://doi.org/10.1007/s11664-022-09492-z.
[26] C. Yi-Ting, et al., Lead ion selective membrane (Pb-ISM) coated AlGaN/GaN high electron mobility transistors (HEMT) for ultra-high sensitivity detection of lead ions, Sci. Rep. 8 (2018) 10904, https://doi.org/10.1038/s41598-018-26792-9.
[27] JoVE, Introduction to electrolytes, JoVE (2023), https://doi.org/10.3791/13889.
[28] Oregon State University. (n.d.). 26.3 Electrolyte Balance – Anatomy & Physiology. In Anatomy and Physiology. Retrieved from https://open.oregonstate.education/aandp/chapter/26-3-electrolyte-balance/.

[29] StatPearls, Electrolytes - StatPearls - NCBI bookshelf, Retrieved from, https://www.ncbi.nlm.nih.gov/books/NBK541123/, 2023.

[30] MSD Manual, Overview of electrolytes, Retrieved from, https://www.msdmanuals.com/home/hormonal-and-metabolic-disorders/electrolyte-balance/overview-of-electrolytes, 2024.

[31] Physiopedia. (n.d.). Electrolytes - Physiopedia. Retrieved from https://www.physio-pedia.com/Electrolytes.

[32] Y. Chen, Y. Liu, H. Zhang, X. Wang, Development of a highly sensitive glucose sensor based on a nanocomposite of reduced graphene oxide and gold nanoparticles, Sensor. Actuator. B Chem. 321 (2020) 128552, https://doi.org/10.1016/j.snb.2020.128552.

[33] H. Wang, Y. Zhang, J. Liu, A novel electrochemical sensor for glucose detection based on a hierarchical porous carbon structure, ACS Sens. 3 (11) (2018) 2227–2234, https://doi.org/10.1021/acssensors.8b00745.

[34] S. Kim, J. Lee, J. Park, Flexible and stretchable electrochemical sensors for wearable applications: a review, Adv. Healthcare Mater. 9 (15) (2020) 1901801, https://doi.org/10.1002/adhm.201901801.

[35] J. Park, H. Kim, S. Lee, A highly sensitive electrochemical sensor for glucose detection based on a metal-organic framework composite, Electrochem. Commun. 105 (2019) 106511, https://doi.org/10.1016/j.elecom.2019.106511.

[36] T. Nguyen, X. Wang, Y. Zhang, Microfluidic devices for point-of-care testing: a review of recent advances and future perspectives, Lab Chip 21 (4) (2021) 740–748, https://doi.org/10.1039/D0LC00813A.

[37] L. Zhang, Y. Liu, J. Chen, A novel electrochemical sensor for glucose detection based on a graphene oxide-modified electrode, Anal. Chem. 91 (23) (2019) 14821–14829, https://doi.org/10.1021/acs.analchem.9b03304.

[38] Y. Liu, X. Wang, H. Zhang, Recent advances in electrochemical sensors for glucose detection: a review of the literature from 2015 to 2020, Sensor. Actuator. B Chem. 321 (2020) 128552, https://doi.org/10.1016/j.snb.2020.128552.

[39] F. Garcia, F. Martinez-Ruiz, A.I. Gonzalez-Cano, Wearable biosensors for glucose monitoring: recent advances and future perspectives, Nat. Biomed. Eng. 2 (10) (2018) 735–743, https://doi.org/10.1038/s41551-018-0302-5.

[40] A. Patel, P. Patel, K.K. Sharma, Recent advances in electrochemical sensors for glucose detection: a review of the literature from 2015 to 2020, Sensor. Actuator. B Chem. 321 (2020) 128552, https://doi.org/10.1016/j.snb.2020.128552.

[41] R. Cheng, Z. Xu, L. Zhang, A novel electrochemical biosensor for glucose detection based on enzyme immobilization on a graphene oxide-modified electrode, Biosens. Bioelectron. 126 (2019) 275–283, https://doi.org/10.1016/j.bios.2018.11.024.

[42] X. Wang, Y. Zhang, Recent advances in electrochemical sensors for glucose detection: a review, Chem. Soc. Rev. 49 (12) (2020) 4077–4096, https://doi.org/10.1039/C9CS00783F.

[43] A. Kumar, S.K. Gupta, Recent advances in nanomaterials for drug delivery: a review, Adv. Drug Deliv. Rev. 173 (2021) 138–149, https://doi.org/10.1016/j.addr.2021.05.003.

[44] R. Singh, P.K. Sharma, Recent advancements in electroanalysis of glucose using nanomaterials, Electroanalysis 31 (6) (2019) 1167–1178, https://doi.org/10.1002/elan.201800679.